

Properties of Zeolite Nanopowder Coated with Titanium Dioxide by Atomic Layer Deposition

Bo Kyung Lee, Hae Ryul Ok, Hye Jin Bae, Hyug Jong Kim and Byung Ho Choi[†]

Department of Materials Science and Engineering Kumoh National Institute of Technology,
Gumi-si 39177, Republic of Korea

(Received December 30, 2015 : Revised January 25, 2016 : Accepted January 28, 2016)

Abstract Nanosized zeolites were prepared in an autoclave using tetraethoxysilane (TEOS), tetrapropylammonium hydroxide (TPAOH), and H₂O, at various hydrothermal synthesis temperatures. Using transmission electron microscopy and particle size analysis, the nanopowder particulate sizes were revealed to be 10-300 nm. X-ray diffraction analysis confirmed that the synthesized nanopowder was silicalite-1 zeolite. Using atomic layer deposition, the fabricated zeolite nanopowder particles were coated with nanoscale TiO₂ films. The TiO₂ films were prepared at 300 °C by using Ti[N(CH₃)₂]₄ and H₂O as precursor and reactant gas, respectively. In the TEM analysis, the growth rate was ~0.7 Å/cycle. Zeta potential and sedimentation test results indicated that, owing to the electrostatic repulsion between TiO₂-coated layers on the surface of the zeolite nanoparticles, the dispersibility of the coated nanoparticles was higher than that of the uncoated nanoparticles. In addition, the effect of the coated nanoparticles on the photodecomposition was studied for the irradiation time of 240 min; the concentration of methylene blue was found to decrease to 48 %.

Key words zeolite, atomic layer deposition, TiO₂, photodecomposition.

1. Introduction

Considerable attention has been devoted to the synthesis of zeolites. Zeolites are micro-porous crystalline materials that are used as catalysts, membranes, and chemical sensors.¹⁻³⁾ The development of functional coatings plays a crucial role in the applications of zeolites to displays, solar cells, and architectural glasses. In this respect, the use of coatings that exhibit high transmittance and anti-bacterial effects could add value to these glasses. In the past decade, however, the development of zeolite nanoparticles that are smaller than 100 nm, in the form of stable colloidal suspensions, was a major achievement in the zeolite science. Much effort has been devoted to synthesize zeolite nanoparticles owing to their technological importance.⁴⁻⁷⁾

In our work, nanosized and porous zeolites have been prepared by using tetraethoxysilane (TEOS), tetrapropylammonium hydroxide (TPAOH), and H₂O, by hydrothermal synthesis at various temperatures. The fabricated zeolite nanopowder particles were coated with TiO₂ films by using

atomic layer deposition. The TiO₂ films were prepared at 300 °C by using Ti[N(CH₃)₂]₄ and H₂O as precursor, and reactant gas, respectively. The effects of the TiO₂ films on the dispersibility of zeolite nanoparticles and photocatalysis were investigated as a function of the coating film thickness.

2. Experimental Procedure

The synthesis-related solutions were prepared by using TEOS (99 %, Aldrich) and TPAOH (1.0 M in water, Aldrich). TEOS was hydrolyzed with an aqueous TPAOH and concentrated to about 30 wt% SiO₂, which resulted in the formation of a viscous clear sol. It was then aged at 80 °C for 10 min. For the fabrication of nanoparticles, the aged sol was then hydrothermally reacted at ~100-170 °C for 2 h. The sol was rinsed, dried, and calcined at 550 °C for 2 h. The TiO₂ films were deposited on the fabricated zeolite nanoparticles by using a vertical flow-type ALD reactor.⁸⁻⁹⁾ The precursor of Ti[N(CH₃)₂]₄ was delivered from a stainless steel container with the carrier

[†]Corresponding author

E-Mail : choibh@kumoh.ac.kr (B. H. Choi, Kumoh Nat'l Univ.)

© Materials Research Society of Korea, All rights reserved.

This is an Open-Access article distributed under the terms of the Creative Commons Attribution Non-Commercial License (<http://creativecommons.org/licenses/by-nc/3.0>) which permits unrestricted non-commercial use, distribution, and reproduction in any medium, provided the original work is properly cited.

of Ar at 70 °C. The delivery lines were maintained at 70 °C to prevent condensation of $\text{Ti}[\text{N}(\text{CH}_3)_2]_4$ inside the lines. The reactor temperature and the working pressure in the reactor were approximately 300 °C and 1 torr, respectively. H_2O was used as a reactant gas and Ar was used as a carrier and purge gas. The opening and closing sequences of the air valves were controlled by using a computer. The ALD process consisted of a given number of identical cycles. The TiO_2 film thickness was controlled by varying the number of ALD cycles.

The size and the distribution of nanoparticles were determined by using a transmission electron microscope (TEM, Jeol, Jem 2100) and particle size analyzer (PSA, Photal, Elsz), respectively. The crystal phases were determined by using an X-ray diffraction analyzer (XRD, Rigaku, X-MAX/2000-PC). The composition of the films coated on the fabricated zeolite particles was examined by using energy dispersive spectroscopy (EDS, Oxford-INCA). The dispersion of the TiO_2 -coated zeolite nanoparticles was confirmed by using a zeta plus potential analyzer (ELS-8000, Otasuka Electronics Co.). The dispersibility of coated and uncoated zeolite nanoparticles in ethanol was also analyzed by performing sedimentation measurements. To confirm the photocatalytic reaction, a thin film metrology tool (F10-VC, Filmetrics) was used for monitoring the absorbance of the methylene blue (1×10^{-5} mole/l) solution at the absorption maximal wavelength of 664 nm, by using UV-lamps (UV-100S, NAWOO)

with the wavelength of ~ 365 nm.

3. Result and Discussion

3.1 Synthesis of the nanoparticles

The TEM images of the fabricated nanoparticles are shown in Fig. 1. As can be seen, the mean diameter of the nanoparticles is ~ 10 nm at the hydrothermal temperature of 100 °C. As the hydrothermal temperature increases up to 170 °C, the mean diameter of the nanoparticles increases up to 300 nm. In addition, the nanoparticles exhibit almost spherical morphology and their size distribution is quite concentrated (the nanoparticles are quite similar to each other), as shown in Fig. 2. The previously reported primary diameter of the nanoparticles was ~ 4 nm, and it increased from ~ 57 nm to ~ 96 nm as the hydrothermal temperature increased from 60 °C to 100 °C.¹⁰⁾

Fig. 3 shows the XRD intensity plot for the fabricated nanoparticles. The peaks at 2θ values of 7.94, 8.90, 23.10, 23.98, 24.61, 29.93, 45.14, and 45.64° correspond to the standard zeolite peaks.¹¹⁾ Therefore, the nanoparticles were confirmed to be the silicalite-1 zeolite.

3.2 TiO_2 ALD coating

Fig. 4 shows the TEM image of a TiO_2 -coated zeolite nanoparticle. The film was deposited by using ALD at a setting of 100 cycles. The TEM image reveals that the

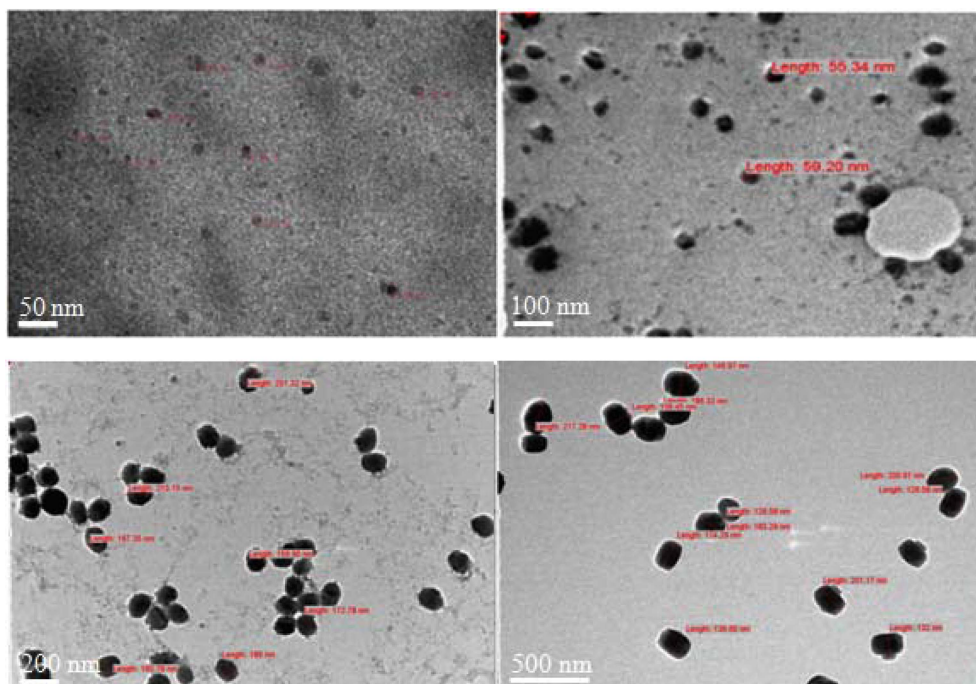


Fig. 1. TEM images of the fabricated nanoparticles, for different hydrothermal synthesis temperatures: (a) 100 °C, (b) 120 °C, (c) 150 °C, and (d) 170 °C.

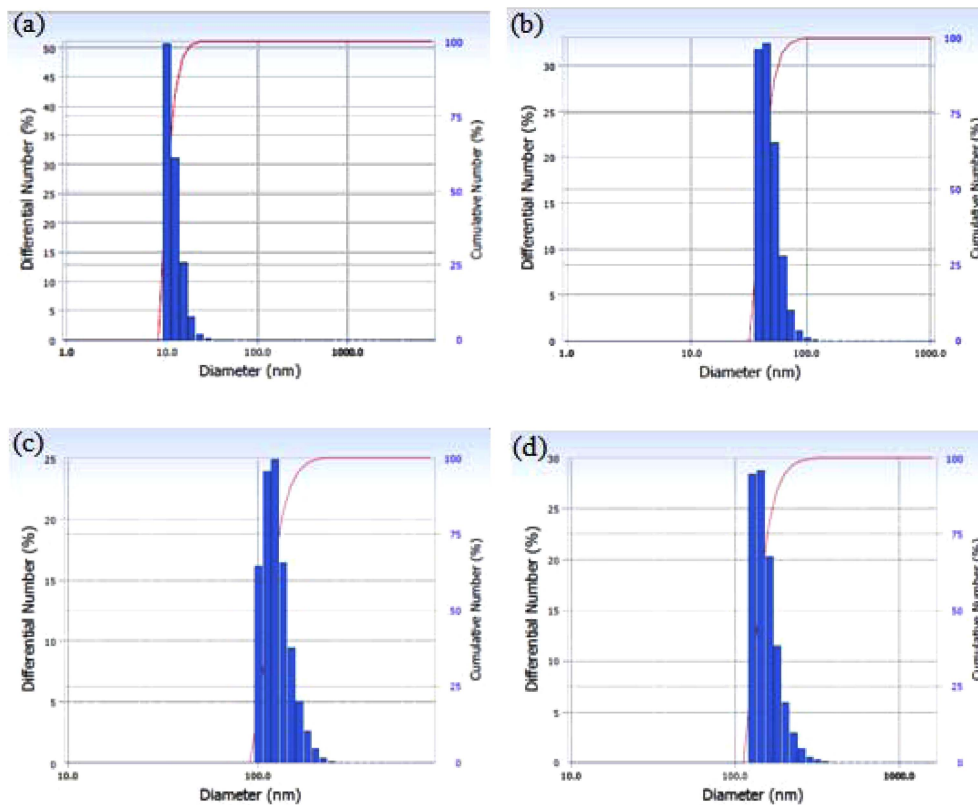


Fig. 2. PSA plots for the fabricated nanoparticles, for different hydrothermal synthesis temperatures: (a) 100 °C, (b) 120 °C, (c) 150 °C, and (d) 170 °C.

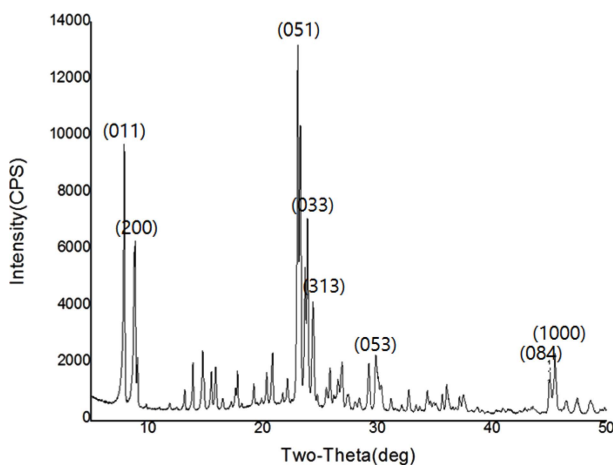


Fig. 3. XRD intensity plot for the fabricated nanoparticles.

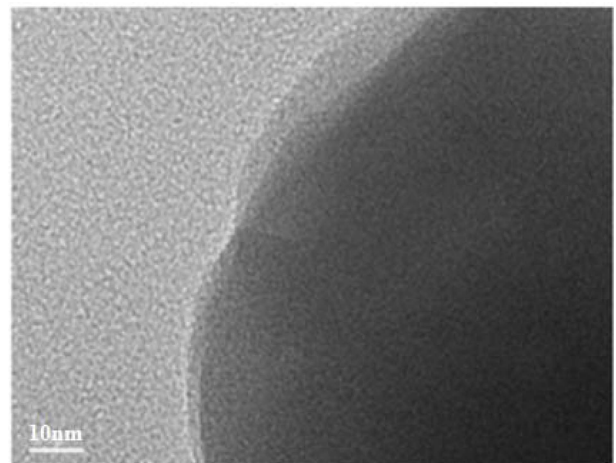


Fig. 4. TEM image of a TiO₂-coated zeolite nanoparticle.

TiO₂ film on this zeolite nanoparticle is continuous and its thickness is ~7 nm. As a result, the growth rate is ~0.7 Å per cycle.

The Zeta potential of the fabricated TiO₂-coated zeolite nanoparticles ranged from -20 mV to ~-47 mV, depending on the number of ALD cycles, as shown in Fig. 5. These values were -11 mV and ~-27 mV lower than the corresponding values for the uncoated zeolite particles.

This implies that the coated nanoparticles are more negatively charged than the uncoated ones. Furthermore, the more negatively charged TiO₂-coated zeolite nanoparticles with higher electrostatic repulsion may yield better particle dispersibility.¹²⁾

The sedimentation test results for the uncoated and coated samples are shown in Fig. 6. For the uncoated samples, the sedimentation occurred in less than 1 h; the

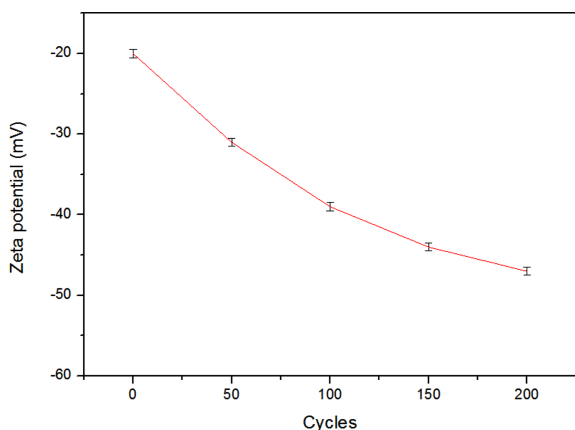


Fig. 5. Zeta potential of the uncoated and TiO₂-coated zeolite particles, as a function of the number of ALD cycles.

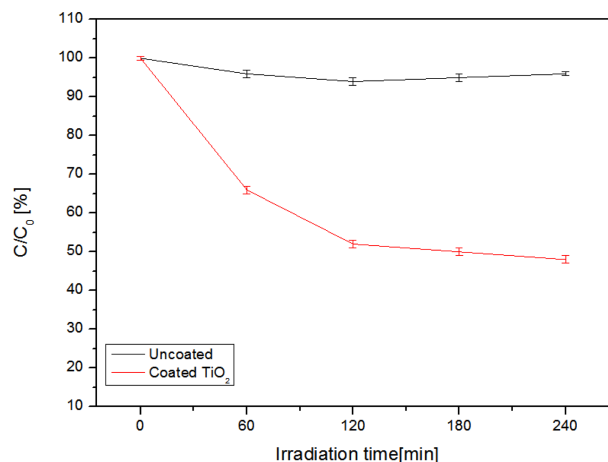


Fig. 7. Decomposition of methylene blue ($C_0 = 1 \times 10^{-5}$ mole/l) under UV irradiation of the TiO₂-coated zeolite nanopowder deposited at 200 cycles.

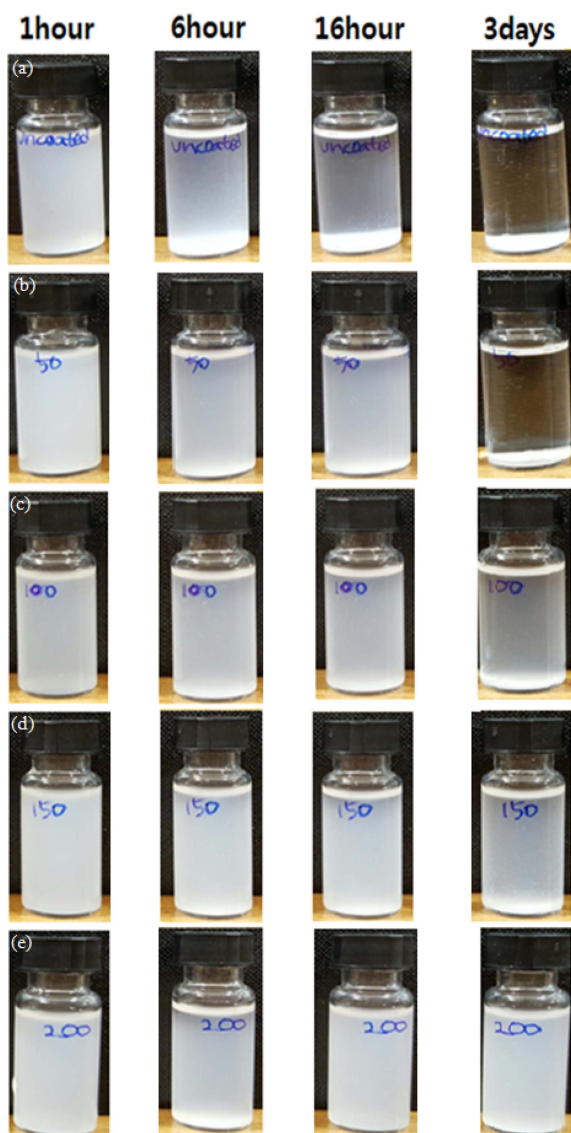


Fig. 6. Sedimentation behavior: (a) uncoated, TiO₂-coated by ALD, (b) 50 cycles, (c) 100 cycles, (d) 150 cycles, and (e) 200 cycles.

supernatant was somewhat turbid and turned into a clear supernatant after additional 6 h. The suspensions separated very quickly into sediments; a clear supernatant atop the sediment is observed in Fig. 6(a). The separation interfaces between the sediment and the liquid were sharp and moved downward with time. In contrast, the dispersion of the coated nanoparticles was much more stable and exhibited stronger dependence on the number of ALD cycles, revealing a different stability. The sedimentation rates for the TiO₂-coated zeolite samples (Figs. 6(d) and (e)) were smaller than that for the uncoated zeolite sample.¹³⁻¹⁶ Even after 6 days, the solution remained turbid. This indicates that the TiO₂ coating of zeolite nanoparticles improved the dispersion stability of zeolite nanoparticles in neutral water.

Fig. 7 shows the photocatalytic decomposition of methylene blue for the uncoated and TiO₂-coated zeolite nanopowder particles. The TiO₂-coated zeolite nanopowder exhibited stronger catalytic properties than the uncoated one. For the irradiation time of 240 min, the concentration of methylene blue decreased down to 48%. In contrast, for the uncoated zeolite nanopowder, the concentration of methylene blue was almost unchanged. The changes in concentration of methylene blue are mainly controlled by the surface adsorption of methylene blue on TiO₂ and the photocatalytic reaction is obvious.¹⁷⁾

4. Conclusion

We successfully demonstrated the synthesis of zeolite nanoparticles. To prevent aggregation, TiO₂ coating was applied to the fabricated nanoparticles by using atomic layer deposition. Particle dispersibility improved with increasing the TiO₂ coating thickness, because the TiO₂

coating imparted the coated zeolite nanoparticles with electrostatic repulsion. The TiO₂ coating films improved the dispersibility of nanoparticles and prevented the nanoparticles from forming aggregates. In addition, the TiO₂-coated zeolite nanopowder exhibited excellent photocatalytic performance.

Acknowledgement

This study was supported by Research Fund, Kumoh National Institute of Technology.

References

1. C.-Y. Hsu, A. S. T. Chiang, R. Selvin and R. W. Thompson, *J. Phys. Chem. B.*, **109**, 18804 (2005).
2. R. Ravishankar, C. E. A. Kirschhock, P.-P. K.-Gerrits, E. J. P. Feijen, P. J. Grobet, P. Vanoppen, F. C. D. Schryver, G. Mieke, H. Fuess, B. J. Schoeman, P. A. Jacobs and J. A. Martens, *J. Phys. Chem. B.*, **103**, 4960 (1999).
3. M. Vilaseca, J. Coronas, A. Cirera, A. Cornet, J. R. Morante and J. Santamaria, *Catal. Today.*, **82**, 179 (2003).
4. A. Beganskiene, S. Sakirzanovas, I. Kazadojev, A. Melninkaitis, V. Sirutkaitis and A. Kareiva, *Mater. Sci. (Poland)*, **25**, 818 (2007).
5. A. Shokuhfar, E. Eghdam and M. Alzamani, *J. Nanosci. Nanotechnol.*, **2**, 22 (2012).
6. G. Wicht, R. Ferrini, S. Schuttel and L. Zuppiroli, *Macromol. Mater. Eng.*, **295**, 628 (2010).
7. A. S. T. Chiang, L.-J. Wong, S.-Y. Li, S.-L. Cheng, C.-C. Lee, K.-L. Chen, S.-M. Chen and Y.-J. Lee, *Stud. Surf. Sci. Catal.*, **170**, 1583 (2007).
8. H. S. Kim, H. J. Kim, Y. K. Jeong, S. H. Kim, S. W. Lee, B. K. Jeong, H. H. Lee and B. H. Choi, *Solid State Phenom.*, **124**, 375 (2007).
9. H. J. Kim, H. G. Kim, I. G. Kang and B.H. Choi, *J. Adv. Phys. Chem.*, **2011**, 4 (2011).
10. Q. Li, D. Creaser and J. Sterte, *Microporous Mesoporous Mater.*, **31**, 141 (1999).
11. M. M. J. Treacy, J. B. Higgins, *Collection of simulated XRD powder patterns for zeolites*, (4th Eds.), Elsevier Science & Technology Books, Amsterdam - London - New York - Oxford - Paris - Shannon - Tokyo, 2001, p. 236-239.
12. Y. Liu, C. Ge, M. Ren, H. Yin, A. Wang, D. Zhang, C. Liu, J. Chen, H. Feng, H. Yao and T. Jiang, *Appl. Surf. Sci.*, **254**, 2809 (2008).
13. Y. Wang, J. Zhang, X. Shen, C. Shi, J. Wu and L. Sun, *Mater. Chem. Phys.* **98**, 217 (2006).
14. H. Tada, O. Nishio, N. Kubo, H. Matsui, M. Yoshihara, T. Kawahara, H. Fukui and S. Ito, *J. Colloid Interface Sci.*, **306**, 274 (2007).
15. X. Xu, M. Oliveira and J. M. F. Ferreira, *J. Colloid Interface. Sci.*, **259**, 391 (2003).
16. M. Sabzi, S. M. Mirabedini, J. Zohuriaan-Mehr and M. Atai, *Prog. Org. Coat.*, **65**, 222 (2009).
17. H. Chang, C. Su, C.-H. Lo, L.-C. Chen, T.-T. Tsung and C.-S. Jwo, *Mater. Trans.*, **45**, 3334 (2004).